



HAL
open science

HepaRG Self-Assembled Spheroids in Alginate Beads Meet the Clinical Needs for Bioartificial Liver

Mattia Pasqua, Ulysse Pereira, Antonietta Messina, Claire de Lartigue,
Pascale Vigneron, Anne Dubart-Kupperschmitt, Cécile Legallais

► **To cite this version:**

Mattia Pasqua, Ulysse Pereira, Antonietta Messina, Claire de Lartigue, Pascale Vigneron, et al.. HepaRG Self-Assembled Spheroids in Alginate Beads Meet the Clinical Needs for Bioartificial Liver. Tissue Engineering: Parts A, B, and C, 2020, 26 (11-12), pp.613-622. 10.1089/ten.tea.2019.0262 . hal-02884175

HAL Id: hal-02884175

<https://hal.science/hal-02884175>

Submitted on 11 Dec 2020

HAL is a multi-disciplinary open access archive for the deposit and dissemination of scientific research documents, whether they are published or not. The documents may come from teaching and research institutions in France or abroad, or from public or private research centers.

L'archive ouverte pluridisciplinaire **HAL**, est destinée au dépôt et à la diffusion de documents scientifiques de niveau recherche, publiés ou non, émanant des établissements d'enseignement et de recherche français ou étrangers, des laboratoires publics ou privés.

Tissue Engineering

Tissue Engineering Manuscript Central: <http://mc.manuscriptcentral.com/ten>

HepaRG self-assembled spheroids in alginate beads meet the clinical needs for bioartificial liver

Journal:	<i>Tissue Engineering</i>
Manuscript ID	TEA-2019-0262
Manuscript Type:	Original Article
Date Submitted by the Author:	26-Sep-2019
Complete List of Authors:	<p>Pasqua, Mattia; Universite de Technologie de Compiegne, UMR CNRS 7338 Biomechanics & Bioengineering Pereira, Ulysse; Universite de Technologie de Compiegne, UMR CNRS 7338 Biomechanics & Bioengineering Messina, Antonietta; Paris-Sud University, Départements Hospitalo-Universitaires (DHU) Hepatinov; Paris-Saclay University, UMR_S1193 Inserm de Lartigue, Claire; Universite de Technologie de Compiegne, UMR CNRS 7338 Biomechanics & Bioengineering Vigneron, Pascale; Universite de Technologie de Compiegne, UMR CNRS 7338 Biomechanics & Bioengineering Dubart-Kupperschmitt, Anne; Paris-Sud University, Départements Hospitalo-Universitaires (DHU) Hepatinov; Paris-Saclay University, UMR_S1193 Inserm Legallais, Cecile; Universite de Technologie de Compiegne, UMR CNRS 7338 Biomechanics & Bioengineering; Paris-Sud University, Départements Hospitalo-Universitaires (DHU) Hepatinov</p>
Keyword:	<p>Liver < Applications in Tissue Engineering (DO NOT select this phrase; it is a header ONLY), Cell Differentiation < Fundamentals of Tissue Engineering (DO NOT select this phrase; it is a header ONLY), 3-D Cell Culture < Enabling Technologies in Tissue Engineering (DO NOT select this phrase; it is a header ONLY), Cell Encapsulation < Enabling Technologies in Tissue Engineering (DO NOT select this phrase; it is a header ONLY), Hydrogels < Enabling Technologies in Tissue Engineering (DO NOT select this phrase; it is a header ONLY)</p>
Manuscript Keywords (Search Terms):	Bioartificial liver, Acute liver failure, HepaRG spheroids, Cell encapsulation, Tissue engineering
Abstract:	<p>In liver tissue engineering, cell culture in spheroids is now well recognized to promote the maintenance of hepatic functions. However, the process leading to spheroids formation is time consuming, costly, and not easy to scale-up for further use in human bioartificial liver (BAL) applications. In this study, we encapsulated HepaRG cells (precursors of hepatocyte-like cells) in alginate 1.5% without pre-forming spheroids. Starting from a given hepatic biomass, we analysed cell differentiation and metabolic performance for further use in fluidized-bed BAL. We observed that cells rearranged as aggregates into the beads and adequately differentiated over time, in the absence of any differentiating factors classically used. At day 14 post-encapsulation, cells displayed a</p>

1
2
3
4
5
6
7
8
9
10
11
12
13
14
15
16
17
18
19
20
21
22
23
24
25
26
27
28
29
30
31
32
33
34
35
36
37
38
39
40
41
42
43
44
45
46
47
48
49
50
51
52
53
54
55
56
57
58
59
60

	large set of hepatic features necessary for the treatment of a patient in acute liver failure. These activities include albumin synthesis, ammonia and lactate detoxification and the efficacy of the enzymes involved in the xenobiotic metabolism (such as CYP1A1/2).

SCHOLARONE™
Manuscripts

HepaRG self-assembled spheroids in alginate beads meet the clinical needs for bioartificial liver

Mattia Pasqua, M.S.,¹ Ulysse Pereira, Ph.D.,¹ Antonietta Messina, Ph.D.,^{2,3} Claire de Lartigue, M.S.,¹
Pascale Vigneron, B.S.,¹ Anne Dubart-Kupperschmitt, M.D.,^{2,3} Cecile Legallais, Ph.D.^{1,2}

¹UMR CNRS 7338 Biomechanics & Bioengineering, Université de technologie de Compiègne, Sorbonne Universités, 60203 Compiègne, France.

²DHU Hépatinov, Villejuif, France.

³UMR_S1193 Inserm / Paris-Saclay University, Villejuif, France.

E-mail addresses and telephone numbers: mattia.pasqua@utc.fr (Mattia Pasqua) +33 3 44 23 44 23, ulysse.pereira@utc.fr (Ulysse Pereira) +33 3 44 23 44 23, antonietta.messina@inserm.fr (Antonietta Messina) +33 3 44 23 44 23, claire.de-lartigue@utc.fr (Claire de Lartigue) +33 3 44 23 44 23, pascale.vigneron@utc.fr (Pascale Vigneron) +33 3 44 23 44 23, anne.dubart@inserm.fr (Anne Dubart-Kupperschmitt) +33 3 44 23 44 23, cecile.legallais@utc.fr (Cecile Legallais) +33 3 44 23 44 23.

Corresponding author:

Cecile Legallais (cecile.legallais@utc.fr), +33 3 44 23 44 23

UMR CNRS 7338 Biomechanics & Bioengineering, Université de technologie de Compiègne, Alliance Sorbonne Université, Rue du Dr Schweitzer, 60203 Compiègne, France

Impact statement

It is recognized that culturing cells in spheroids is advantageous since they better recapitulate the three-dimensional physiological microenvironment. This approach can be exploited in bioartificial liver applications, where getting a functional hepatic biomass is the major pitfall. Our study describes an original method of culturing hepatic cells in alginate beads that allows the autonomous formation of spheroids after three days of culture. In turn, cells adequately differentiate and display a large set of hepatic features. They are also able to treat a model of pathological plasma. Finally, this setup can be easily scaled-up for the treatment of acute liver failure.

1. Introduction

Fulminant liver failure is a life-threatening critical illness with an extremely high mortality rate, even if intensive care is provided (1). To date, liver transplantation is the only available treatment for patients with end-stage liver disease such as acute liver failure (ALF) (2). The growing gap between the number of patients on waiting list and the number of donor organs available has highlighted the need for alternative therapies as a bridge to transplantation or liver regeneration. Extracorporeal liver support systems could represent a valid solution for this problematic and nowadays two types of devices are considered: artificial (ALs) and bioartificial liver support systems (BALs). ALs are designed to remove water-soluble toxins from patient's plasma in order to improve clinical state (3) while BALs are meant to fulfil the maximum number of synthetic and detoxification liver functions (4). The key component of a BAL is the bioreactor, the cell-housing component. Its expected role is to allow a patient in ALF to survive until an available liver donor or to stimulate autonomous liver regeneration.

Access to a bioactive mass (or biomass) is the main pitfall in the context of human BALs. Although primary human hepatocytes are still considered the gold standard, their limited availability, the phenotypic instability (5), as well as logistical issues, hamper their use in BALs. In the past, most of the BALs in clinical or preclinical studies relied on primary porcine hepatocytes, due to their easy availability and high functional activities (6)(7)(8). However, transfer of zoonotic diseases (9), protein-protein incompatibility between species and possible immune responses generated during treatment remain challenges for the use of xenogeneic hepatocytes (10). Recently, the focus has been put on the use of induced pluripotent stem cells and embryonic stem cells as innovative cell source for BAL, especially for their great proliferative capacity and their potential to show metabolic functions close to those of human hepatocytes. Despite great efforts in this direction, today these cell types are not able yet to exhibit full functions of mature hepatocytes in terms of metabolic performance and efforts have still to be made to allow their clinical use (11).

Currently, human cell lines keep thus a great potential for BAL application. The main advantages of hepatocyte cell lines are their almost unlimited proliferative capacity and the relatively cheap culture process. They demonstrate some metabolic functionalities comparable to human hepatocytes and also to be safe and non-tumorigenic (12). HepG2 and its sub-clone present limited metabolic functions (5)

1
2
3 for BAL applications, although encouraging results were recently presented by the group of Selden on
4 a pig model of ALF. HepaRG is a hepatic progenitor cell line able to differentiate into hepatocyte-like
5 cells after 14 days of specific culture (13). Investigators already demonstrated that HepaRG cell line
6 was suitable for BAL application for their proliferation capacity and their enhanced hepatic metabolism
7 in three-dimensional (3D) configuration (14).
8
9

10
11
12
13 In the context of BAL, hepatic cell microencapsulation in alginate porous beads has been recognized as
14 an interesting alternative to classical cell immobilization in hollow fibre membranes. This material is
15 quite inert, not toxic regarding cells and ensures an adequate biocompatibility. In addition, its relatively
16 low cost and gelation capacity by divalent cations such as Ca^{2+} makes the process suitable for hepatocyte
17 encapsulation (15). In vitro liver models combined with tissue engineering approaches provide a 3D
18 microenvironment which can be expected to mimic in vivo conditions. In the process of encapsulation,
19 cells are entrapped within spherical alginate microbeads that protect them from mechanical stress while
20 ensuring exchanges of nutrients or waste molecules within the surrounding medium. The immuno-
21 isolation provided by alginate encapsulation is undoubtedly the major advantage of this technology (16).
22 For BAL application, the challenge is to induce/maintain the hepatic functions over time starting from
23 an initial biomass, taking into account parameters such as costs, manipulation ease for the operator, and
24 scaling-up feasibility. Recently, some authors successfully enhanced biosynthetic and xenobiotic
25 performance of HepaRG functions, cultivating cells as spheroids (SPHs) before encapsulation, without
26 the use of dimethyl sulfoxide (DMSO) (17). Nevertheless, the technologies available nowadays for the
27 production of large amounts of spheroids (such as rotating or shaking reactors) may lead to an
28 unacceptable loss of cells that reduces considerably the initial biomass. Indeed, the majority of these
29 studies are focused on toxicology approaches in which it is important to evaluate the metabolic activity
30 “per cell”. In the context of BAL, the challenge is not to determine the best activity “per cell” but rather
31 “per bioreactor”, taking into account logistic hurdles or costs due to additional manipulation.
32
33

34
35
36
37
38
39
40
41
42
43
44
45
46
47
48
49
50
51
52
53
54 Therefore, in this study we propose to analyse cell differentiation and metabolic performance of an
55 initial biomass of encapsulated HepaRG in alginate 1.5%, for further use in fluidized-bed BAL.
56
57
58
59
60

2. Materials and Methods

2.1. 2D cell culture

HepaRG from Biopredic (Rennes, France) cells were expanded in two-dimensional (2D) monolayers following the indications reported by the supplier. Cells were passaged every 2 weeks until passage 18, with proliferation culture medium William's E (WE, with sodium bicarbonate, without L-glutamine and phenol red, Sigma-Aldrich, with added Biopredic 710 proliferation media) replenishment thrice a week. The cultures were maintained in a humidified environment at 37°C, 5 % CO₂. After that, cells were detached by trypsin-ethylenediaminetetraacetic acid (EDTA) 0.25% (ThermoFisher scientific) from the culture flasks and used for the cell encapsulation process (explained in paragraph 2.2).

2.2. Alginate microencapsulation

Cells were encapsulated in alginate (Manucol LKX from FMC BioPolymer) 1.5% (w/v), sterilized by successive filtrations (0.8, 0.45, and 0.22 μm pore size membrane filters). The encapsulation was performed with a home-made system based on a coaxial air flow extrusion method (18). Briefly, the alginate solution containing cells was extruded through a 24 G nozzle and the droplets fell into a gelation bath (NaCl 154 mM, HEPES 10 mM and CaCl₂ 115 mM, pH 7.4). Droplets produced were allowed to settle for 15 min in the gelation bath to ensure gel formation. After that, the microbeads were washed three times in WE medium and then resuspended in proliferation culture media. Finally, the encapsulated cells were transferred in culture dishes and maintained for 14 days in continuous orbital shaking (60 rpm) in a humidified environment at 37 °C, 5 % CO₂. Proliferation culture medium was replaced every 2 days. Empty microbeads (without cells) were also produced as control for the following metabolic tests.

2.3. Cell aggregates diameter measurement

The diameter of the cellular aggregates was determined by measuring their diameter using ImageJ software version 1.52h. For each experiment, the diameter of 10 aggregates in different beads was measured orthogonally by optical microscopy. Mean and standard deviation were calculated.

2.4. Cell performance experimental setup

1
2
3 The experimental setup designed to assess cell metabolic performance is shown in figure 1. At day 0,
4 cells were encapsulated in alginate 1.5%. Cell differentiation was studied via immunofluorescence
5 staining (paragraph 2.6) at day 0, 7, 10 and 14 post-encapsulation and metabolic test (albumin synthesis)
6 between days 0-1, 6-7, 9-10, 13-14 post-encapsulation. At day 7 and 14 post-encapsulation, the cell
7 performance was tested through metabolic and xenobiotic tests. The latter were conducted in intervals
8 of up to 2 hours of incubation and, at each time-point (time 0 and time 2 hours), aliquots of supernatant
9 were collected for further analysis. At the end of each experiment, microbeads were recovered and
10 assessed for cell viability. The quantity of marker analysed was calculated and normalized by the number
11 of hours of incubation and the number of cells seeded. Moreover, in order to avoid artefacts, all the
12 metabolic activities tested were normalized by the quantity at time zero and the control (empty
13 microbeads).
14
15
16
17
18
19
20
21
22
23
24
25
26
27

28 In order to study the differentiation of cells, at day 0, 7, 10, and 14 post-encapsulation the subcellular
29 localization of proteins typically expressed by hepatoblasts and mature hepatocytes was assessed by
30 immunofluorescence (figure 4). At day 0 post-encapsulation, hepatoblasts are present since we observe
31 their typical markers such as AFP, HNF 6 and CK-19. During the differentiation process, the level of
32 hepatoblasts markers decreases while the mature hepatocytes markers show up (ALB, HNF 4 α). The
33 CYP 3A4 is constantly expressed and functional at day 7 and 14. Those qualitative observations are
34 recapitulated in table 2. In parallel, synthesis of albumin remains overall stable over 14 days of culture
35 with a tendency to increase at day 10 (data not shown).
36
37
38
39
40
41
42
43
44

45 3. Discussion

46 In this study, we analysed the metabolic activities of a biomass of micro-encapsulated HepaRG for
47 subsequent treatment of acute liver failure. Such engineered liver tissues could be used in fluidized-bed
48 BAL, a technology developed in our laboratory and in others (25). With a similar bioreactor hosting
49 HepG2 grown in alginate beads, Selden's group recently published the improvements of clinical
50 parameters in a surgical porcine model of liver failure (26). Zhou et al., 2016 also obtained prolonged
51 survival time for pigs with D-galactosamine induced ALF using a fluidized bed BAL hosting porcine
52 primary hepatocytes encapsulated in alginate-chitosan beads.
53
54
55
56
57
58
59
60

1
2
3 As stated in the introduction, further clinical applications request the production of large amounts of
4 encapsulated cells to get a functional and cost effective biomass at human scale. The required hepatic
5 cells' functions are mainly protein synthesis (albumin and clotting factors), ammonia and lactate
6 elimination (both implicated in hepatic encephalopathy and cerebral oedema), xenobiotic detoxification
7 (enzyme machinery involved in cleaning toxins accumulating during ALF) (5). In the present study, we
8 demonstrated that HepaRG microencapsulated in alginate beads were able to produce albumin, detoxify
9 ammonia and lactate, and to express the enzymes involved in the xenobiotic machinery, with highest
10 activity at day 14.

11
12 Our results show that cell viability was affected neither by the encapsulation process nor by the long-
13 time culture cells, nor by the exposition to a toxic culture media, containing typical ALF toxins.
14 Interestingly, within the alginate microbeads, cells were able to rearrange forming cell spheroids, a
15 phenomenon already observed with HepG2/C3A that are highly proliferative (28) (29). In addition,
16 mature hepatocytes markers were present, demonstrating that, when encapsulated, these progenitor cells
17 were able to fully differentiate over time, in the absence of differentiation agents such as growth factors
18 or DMSO, that are classically employed in vitro. The 3D reorganization and the alginate environment
19 are thus promoting cell differentiation in contrast with 2D culture.

20
21 Regarding cells functions, we performed a large set of assessment. It is of note that encapsulated
22 HepaRG are responsive to the ICG tests. The uptake of this dye is carried out by the transporters
23 OATP1B3 and NTCP that are expressed at the basolateral plasma membrane of hepatocytes (20) and
24 excretion is regulated by the transporters MDR3 and MRP2 (21), expressed in the hepatocytes apical
25 (canalicular) membrane (30). Moreover, F-actin accumulating at cellular junctional sites of the cell
26 aggregates resembled interconnected bile canalicular structures. This observation has also been noticed
27 by Rebelo et al., 2014. Both facts indicate a highly polarized cellular organization favouring cell
28 maturation (31). Cell aggregates' dimension increased over the days of culture but remained in a range
29 (maximum 120 μm) where mass transfer was not affected, and where oxygen gradient can take place
30 (32). In addition, it has been observed that when HepaRG in 2D configuration are cultured in orbital
31 shaking, hepatic differentiation and metabolic functions are both positively affected due to higher
32 mitochondrial biogenesis (33). Also in our experimental setup, the encapsulated cells are kept in orbital
33
34
35
36
37
38
39
40
41
42
43
44
45
46
47
48
49
50
51
52
53
54
55
56
57
58
59
60

1
2
3 shaking. These last two phenomena described could induce a gain of function in the whole cell metabolic
4 performances that can explain why some of our activities are stronger in comparison with other authors.
5

6
7 The group of Chamuleau seeded HepaRG in the Amsterdam Medical Center Bioartificial Liver (AMC-
8 BAL), a membrane based bioreactor in which cells are in direct contact with plasma. They reported
9 ammonia (around 0.04 nmol/h/10⁶) and lactate (around 9.3 nmol/h/10⁶) detoxification with lower rates
10 in comparison with our results (respectively 119±20 nmol/h/10⁶ and 167±24 nmol/h/10⁶). These
11 differences can be explained by the fact that in our system cells formed spheroids, on the one hand, and
12 are protected from the shear stress by the alginate structure, on the other hand. In addition, these data
13 were obtained with total plasma and the authors suspected that large molecules in plasma could have a
14 deleterious effect on cells' functions (34). Compared to HepG2/C3A, we can observe that albumin
15 production was in the order of magnitude, and that all phases of enzymatic biodegradation were present,
16 although they are lower than those of primary human hepatocytes just after their collection. Considering
17 Selden's promising results in preclinical studies with HepG2, the same could be expected with HepaRG.
18 As a cell line, issued from hepatocarcinoma, the same protection should be envisaged for safety use in
19 patients, such as the presence of filters downstream the bioreactor (26).
20
21
22
23
24
25
26
27
28
29
30
31
32
33

34 Going back to the encapsulation process, Rebelo et al., 2014 also entrapped HepaRG in alginate beads,
35 with reported high performances regarding biotransformation, interesting toxicological issues.
36 However, they encapsulated pre-formed spheroids and not individual cells, as proposed in the present
37 work. When encapsulating a biomass for long time cultures, it is important to consider different
38 logistical parameters influencing the whole process of manipulation for a future scaling-up for clinical
39 BAL application. From our own experience (Supplementary data), we observed a loss of cells when
40 preparing aggregates/spheroids before encapsulation, especially using processes that can be upscaled
41 such as rotating or shaking reactors. This loss is limited with hanging drop or microfluidic techniques
42 (35), but these latter cannot treat billions of cells as requested for a human BAL size. In addition,
43 aggregates pre-formation request at least 3 days of specific culture, before encapsulation, and additional
44 handling that make the GMP production more complex and not cost-effective. As our preliminary results
45 did not show any evidence of better performances of encapsulated pre-formed HepaRG spheroids, we
46
47
48
49
50
51
52
53
54
55
56
57
58
59
60

1
2
3 conclude that their self-reorganization with alginate beads with appropriate density should be preferred
4
5 in a clinical application strategy.
6

7 In conclusion, in this study we demonstrated that HepaRG cells were able to self-organize as spheroids
8
9 when entrapped in 1.5% alginate beads. After 14 days of culture, these encapsulated cells presented a
10
11 wide range of functions (protein synthesis, enzymatic activities and biotransformation of toxins) that are
12
13 in the range or above those presented in other studies about bioartificial liver. Waiting for fully mature
14
15 hepatic cells issued from pluripotent stem cells, this HepaRG based bioconstruct demonstrated its
16
17 potential for further use for extracorporeal treatment of acute liver failure. The next step will thus be to
18
19 characterize the biomass activity in fluidized-bed BAL, a setup known to favour the mass exchange
20
21 between the plasma of a patient in ALF and the immobilized cells.
22
23
24
25

26 **4. Acknowledgement**

27 We thank Baptiste Hirsinger, Marwa Hussein and Augustin Lerebours for their technical assistance.

28
29 The HepaRG cell line, media and supplements used for this investigation has been supported by
30
31 Biopredic International (funded by ANR 16-RHUS-0005 in the framework of iLite program), for which
32
33 the authors express their appreciation. This cell line has been patented by Inserm, under the number WO
34
35 03/004627.
36
37
38
39
40

41 **5. Disclosure Statement**

42 No competing financial interests exist.
43
44
45
46

47 **6. Funding**

48 This work was supported by PIA-RHU iLite (ANR 16-RHUS-0005)
49
50
51
52
53

54 **7. References**

- 55
56 1. Tuñón MJ, Alvarez M, Culebras JM, González-Gallego J. An overview of animal models for
57
58 investigating the pathogenesis and therapeutic strategies in acute hepatic failure. *World J.*
59
60 *Gastroenterol.* **15**(25), 3086, 2009

- 1
2
3 2. Starokozhko V, Groothuis GMM. Challenges on the road to a multicellular bioartificial liver. *J.*
4
5 Tissue Eng. Regen. Med. **12**(1), e227, 2018
6
- 7 3. Pless G. Artificial and bioartificial liver support. *Organogenesis* [Internet]. **3**(1), 20, 2007
8
- 9 4. Carpentier B, Gautier A, Legallais C. Artificial and bioartificial liver devices: Present and future.
10
11 *Gut*. **58**(12), 1690, 2009
12
- 13 5. van Wenum M, Chamuleau RA, van Gulik TM, Siliakus A, Seppen J, Hoekstra R. Bioartificial
14
15 livers in vitro and in vivo: tailoring biocomponents to the expanding variety of applications.
16
17 *Expert Opin. Biol. Ther.* **14**(12), 1745, 2014
18
- 19 6. Mazariegos G V, Patzer JF, Lopez RC, Giraldo M, DeVera ME, Grogan TA, et al. First Clinical
20
21 Use of a Novel Bioartificial Liver Support System (BLSS)†. *Am. J. Transplant.* Munksgaard
22
23 International Publishers; **2**(3), 260, 2002
24
- 25 7. Mundt A, Puhl G, Muller A, Sauer IM, Muller C, Richard R, et al. A method to assess
26
27 biochemical activity of liver cells during clinical application of extracorporeal hybrid liver
28
29 support. *Int. J. Artif. Organs.* Wichtig Publishing; **25**(6), 542, 2008
30
31
- 32 8. Van De Kerkhove MP, Di Florio E, Scuderi V, Mancini A, Belli A, Bracco A, et al. Phase I
33
34 clinical trial with the AMC-bioartificial liver. *Int. J. Artif. Organs.* **25**(10), 950, 2002
35
- 36 9. Yang Q, Liu F, Pan XP, Lv G, Zhang A, Yu CB, et al. Fluidized-bed bioartificial liver assist
37
38 devices (BLADs) based on microencapsulated primary porcine hepatocytes have risk of porcine
39
40 endogenous retroviruses transmission. *Hepatol. Int.* **4**(4), 757, 2010
41
42
- 43 10. Te Velde AA, Flendrig LM, Ladiges NCJJ, Chamuleau RAFM. Immunological Consequences
44
45 of the use of Xenogeneic Hepatocytes in a Bioartificial Liver for Acute Liver Failure. *Int. J. Artif.*
46
47 *Organs.* SAGE Publications; **20**(4), 229, 1997
48
- 49 11. Chen C, Soto-Gutierrez A, Baptista PM, Spee B. Biotechnology Challenges to In Vitro
50
51 Maturation of Hepatic Stem Cells. *Gastroenterology* [Internet]. The American
52
53 Gastroenterological Association; **154**(5), 1258, 2018
54
- 55 12. Chamuleau R a FM, Poyck PPC, van de Kerkhove M-P. Bioartificial liver: its pros and cons.
56
57 *Ther. Apher. Dial.* **10**(2), 168, 2006
58
- 59 13. Gripon P, Rumin S, Urban S, Le Seyec J, Glaise D, Cannie I, et al. Nonlinear partial differential
60

- equations and applications: Infection of a human hepatoma cell line by hepatitis B virus. Proc. Natl. Acad. Sci. **99**(24), 15655, 2002
14. Hoekstra R, Nibourg GAA, Van Der Hoeven T V., Ackermans MT, Hakvoort TBM, Van Gulik TM, et al. The HepaRG cell line is suitable for bioartificial liver application. Int. J. Biochem. Cell Biol. Elsevier Ltd; **43**(10), 1483, 2011
 15. Legallais C, Kim D, Mihaila SM, Mihajlovic M, Figliuzzi M, Bonandrini B, et al. Bioengineering Organs for Blood Detoxification. Adv. Healthc. Mater. **1800430**, 1, 2018
 16. Tran NM, Dufresne M, Helle F, Hoffmann TW, Francois C, Brochot E, et al. Alginate hydrogel protects encapsulated hepatic HuH-7 cells against hepatitis C virus and other viral infections. PLoS One. **9**(10), 16, 2014
 17. Rebelo SP, Costa R, Estrada M, Shevchenko V, Brito C, Alves PM. HepaRG microencapsulated spheroids in DMSO-free culture: novel culturing approaches for enhanced xenobiotic and biosynthetic metabolism. Arch. Toxicol. **89**(8), 1347, 2014
 18. Gautier A, Carpentier B, Dufresne M, Vu Dinh Q, Paullier P, Legallais C. Impact of alginate type and bead diameter on mass transfers and the metabolic activities of encapsulated c3a cells in bioartificial liver applications. Eur. Cells Mater. **21**(0), 94, 2011
 19. Gabriel E, Schievenbusch S, Kolossov E, Hengstler JG, Rotshteyn T, Bohlen H, et al. Differentiation and Selection of Hepatocyte Precursors in Suspension Spheroid Culture of Transgenic Murine Embryonic Stem Cells. PLoS One. **7**(9), 2012
 20. Graaf W De, Häusler S, Heger M, Ginhoven TM Van, Cappellen G Van, Bennink RJ, et al. Transporters involved in the hepatic uptake of and indocyanine green Tc-mebrofenin. J. Hepatol. [Internet]. European Association for the Study of the Liver; **54**(4), 738, 2011
 21. Cusin F, Azevedo LF, Bonnaventure P, Desmeules J, Daali Y, Pastor CM. Hepatocyte Concentrations of Indocyanine Green Reflect Transfer Rates Across Membrane Transporters. 171, 2017
 22. Diaz GJ. Basolateral and canalicular transport of xenobiotics in the hepatocyte: A review. Cytotechnology. **34**(3), 225, 2000
 23. Sakai Y, Tanaka T, Fukuda J, Nakazawa K. Alkoxyresorufin O-dealkylase assay using a rat

- 1
2
3 hepatocyte spheroid microarray. *J. Biosci. Bioeng.* [Internet]. The Society for Biotechnology,
4 Japan; **109**(4), 395, 2010
- 5
6
7 24. Nibourg GAA, Chamuleau RAFM, van der Hoeven T V., Maas MAW, Ruiters AFC, Lamers
8 WH, et al. Liver progenitor cell line HepaRG differentiated in a bioartificial liver effectively
9 supplies liver support to rats with acute liver failure. *PLoS One.* **7**(6), 1, 2012
- 10
11
12
13 25. Legallais C, Doré E, Paullier P. Design of a fluidized bed bioartificial liver. *Artif. Organs.* **24**(7),
14 519, 2000
- 15
16
17 26. Selden C, Bundy J, Erro E, Puschmann E, Miller M, Kahn D, et al. A clinical-scale BioArtificial
18 Liver, developed for GMP, improved clinical parameters of liver function in porcine liver failure.
19 *Sci. Rep.* **7**(1), 1, 2017
- 20
21
22
23 27. Zhou P, Shao L, Zhao L, Lv G, Pan X, Zhang A, et al. Efficacy of Fluidized Bed Bioartificial
24 Liver in Treating Fulminant Hepatic Failure in Pigs: A Metabolomics Study. *Sci. Rep. Nature*
25 *Publishing Group;* **6**(May), 1, 2016
- 26
27
28
29 28. Coward SM, Selden C, Mantalaris A, Hodgson HJF. Proliferation rates of HepG2 cells
30 encapsulated in alginate are increased in a microgravity environment compared with static
31 cultures. *Artif. Organs.* **29**(2), 152, 2005
- 32
33
34
35 29. Capone SH, Dufresne M, Rechel M, Fleury MJ, Salsac AV, Paullier P, et al. Impact of Alginate
36 Composition: From Bead Mechanical Properties to Encapsulated HepG2/C3A Cell Activities for
37 In Vivo Implantation. *PLoS One.* **8**(4), 2013
- 38
39
40
41 30. Oude Elferink, R.P.J., Coen E. Function and pathophysiological importance of ABCB4. **11**, 601,
42 2007
- 43
44
45
46 31. Blau BJ, Miki T. The role of cellular interactions in the induction of hepatocyte polarity and
47 functional maturation in stem cell-derived hepatic cells. *Differentiation* [Internet]. Elsevier B.V.;
48 **106**(January), 42, 2019
- 49
50
51
52 32. Leedale J, Colley HE, Gaskell H, Williams DP, Bearon RN, Chadwick AE, et al. In silico-guided
53 optimisation of oxygen gradients in hepatic spheroids. *Comput. Toxicol. Elsevier;* **12**(December
54 2018), 100093, 2019
- 55
56
57
58 33. Adam AAA, van der Mark VA, Donkers JM, Wildenberg ME, Oude Elferink RPJ, Chamuleau
59
60

1
2
3 RAFM, et al. A practice-changing culture method relying on shaking substantially increases
4 mitochondrial energy metabolism and functionality of human liver cell lines. PLoS One. **13**(4),
5
6
7 1, 2018
8

9
10 34. Van Wenum M, Chamuleau R, Jongejan A, Treskes P, Meisner S, Hendriks E, et al. Effects of
11 Healthy- and Acute Liver Failure Plasma on Differentiated Human Heparg Progenitor Cells in
12 Monolayers and Bioartificial Livers. J. Hepatol. Elsevier B.V.; **64**(2), S308, 2016
13
14

15
16 35. Mehta G, Hsiao AY, Ingram M, Luker GD, Takayama S. Opportunities and challenges for use
17 of tumor spheroids as models to test drug delivery and efficacy. J. Control. Release. **164**(2), 192,
18
19
20 2012
21

22 Cecile Legallais (cecile.legallais@utc.fr), +33 3 44 23 44 23
23

24 UMR CNRS 7338 Biomechanics & Bioengineering, Université de technologie de Compiègne, Alliance
25
26 Sorbonne Université, Rue du Dr Schweitzer, 60203 Compiègne, France
27
28
29
30
31
32
33
34
35
36
37
38
39
40
41
42
43
44
45
46
47
48
49
50
51
52
53
54
55
56
57
58
59
60

Table 1: list of antibodies

Protein	Reference	Type
AFP (alpha-fetoprotein)	SC 8399	mouse monoclonal IgG
ALB (albumin)	Sigma A6684	mouse monoclonal IgG
CK-19 (cytokeratin 19)	DAKO M0888	mouse monoclonal IgG
CYP3A4 (cytochrome P450 3A4)	SC 53850	mouse monoclonal IgG
HNF 4 α (hepatocyte nuclear factor 4 α)	SC 8987	rabbit polyclonal IgG
HNF 6 (hepatocyte nuclear factor 6)	SC 13050	rabbit polyclonal IgG

Table 2: evolution of cell differentiation over time

Cell state	Marker	Day 0	Day 7	Day 10	Day 14
Hepatoblasts	HNF 6				
	CK-19				
	AFP				
Mature Hepatocytes	HNF 4 α				
	ALB				
	CYP 3A4				

Legend: increasing expression, decreasing expression, constant expression

1
2
3
4
5
6
7
8
9
10
11
12
13
14
15
16
17
18
19
20
21
22
23
24
25
26
27
28
29
30
31
32
33
34
35
36
37
38
39
40
41
42
43
44
45
46
47
48
49
50
51
52
53
54
55
56
57
58
59
60

For Peer Review ONLY / Not for Distribution

1
2
3 Figure Legend
4
5

6 Fig. 1 experimental setup (see text for the details of the protocol)
7

8 Fig. 2 beads morphology (bright field microscopy) and cell viability (confocal microscopy). In
9 green (Calcein AM): viable cells, in red (ethidium homodimer-1): dead cells, in blue (Hoechst
10 33342 dye): cell nuclei. Scale bar: 100 μm
11

12
13 Fig. 3 cells self-rearranged in aggregates: diameters over time (A). F-actin (phalloidin, in green)
14 and nuclei (DAPI, in blue) staining at day 14 (B) (confocal microscopy). Scale bar: 20 μm
15

16
17 Fig. 4 immunofluorescence staining over time (confocal microscopy). Hepatoblast markers (Hb):
18 HNF 6 in red, CK-19 in green, AFP in green, nuclei in blue. Mature hepatocyte markers (MH):
19 HNF 4 α in red, ALB in green, CYP 3A4 in green, nuclei in blue. Scale bar: 20 μm
20

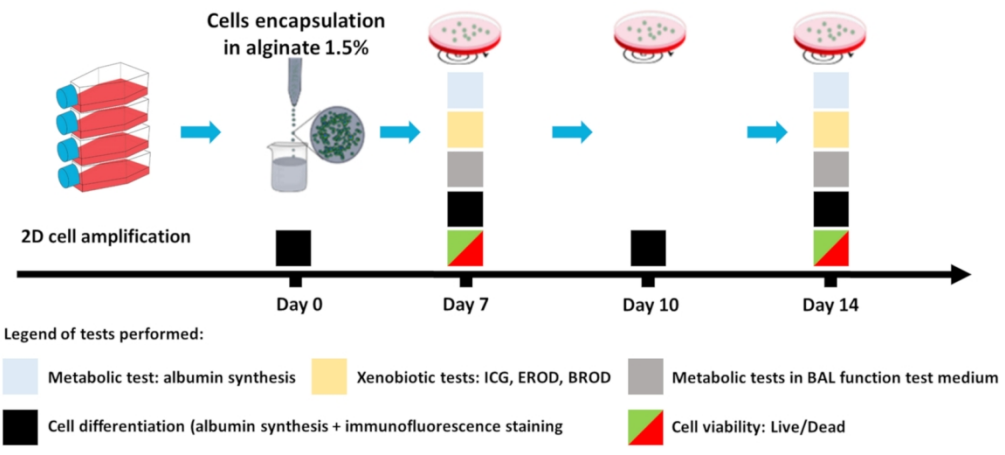
21
22 Fig. 5 metabolic activities of encapsulated cells at day 7 and day 14. Albumin secretion rate (A,
23 significance analysed by Wilcoxon matched-pairs signed-ranks test), ICG releasing rate by the
24 transporters MDR3 and MRP2 (B), CYP1A1/2 activity (C), CYP3A4 activity (D)
25

26
27 Fig. 6 CYP1A1/2 activity after induction by β -naphthoflavone 100 μM and rifampicin 10 μM at
28 day 7 (A) and 14 (B), significance analysed by Mann-Whitney Test
29

30
31 Fig. 7 metabolic activities of encapsulated cells in BAL function test medium at day 7 and 14.
32 Albumin synthesis rate (A), ammonia (B) and lactate (C) detoxification rate
33

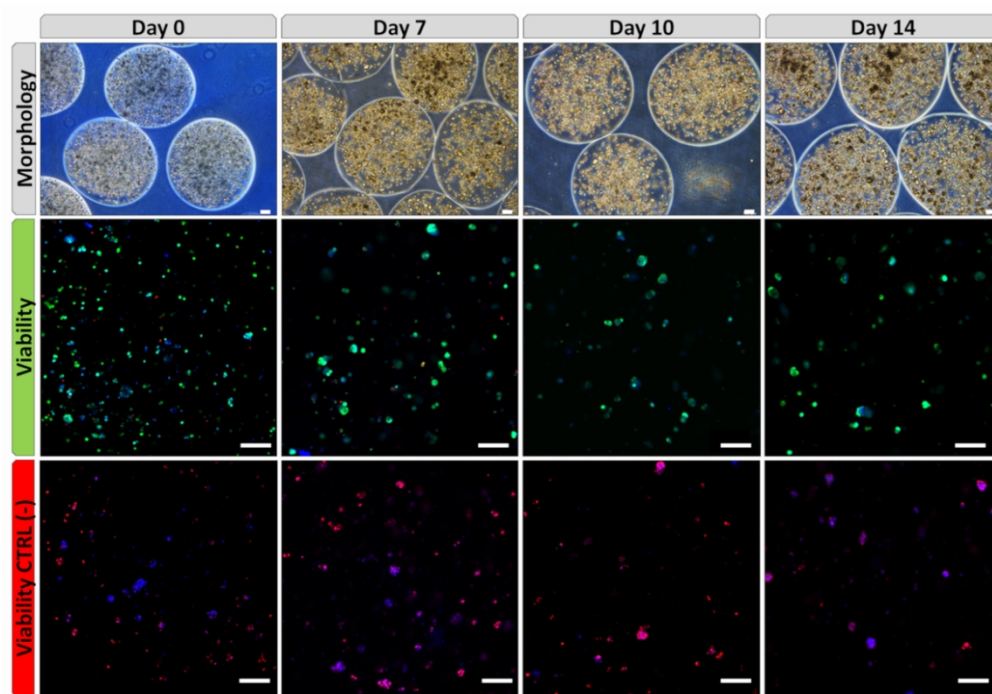
34
35 Fig. 8 cell viability after exposition to BAL function test medium at day 7 and 14 (confocal
36 microscopy). In green (Calcein AM): viable cells, in red (ethidium homodimer-1): dead cells, in
37 blue (Hoechst 33342 dye): cell nuclei. Scale bar: 100 μm
38
39
40
41
42
43
44
45
46
47
48
49
50
51
52
53
54
55
56
57
58
59
60

1
2
3
4
5
6
7
8
9
10
11
12
13
14
15
16
17
18
19
20
21
22
23
24
25
26
27
28
29
30
31
32
33
34
35
36
37
38
39
40
41
42
43
44
45
46
47
48
49
50
51
52
53
54
55
56
57
58
59
60



experimental setup (see text for the details of the protocol)

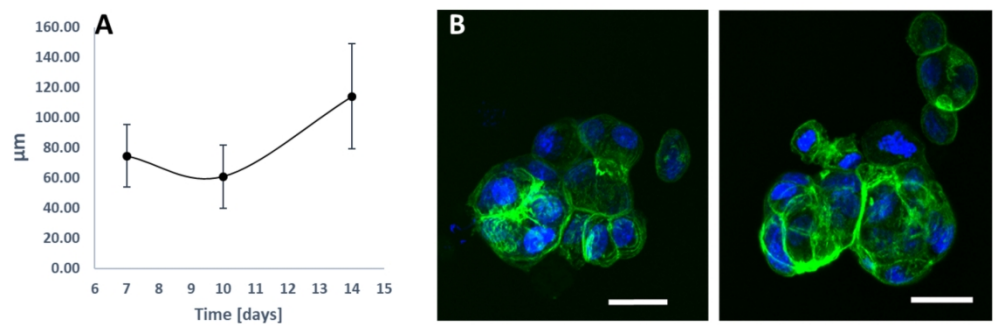
139x62mm (300 x 300 DPI)



beads morphology (bright field microscopy) and cell viability (confocal microscopy). In green (Calcein AM): viable cells, in red (ethidium homodimer-1): dead cells, in blue (Hoechst 33342 dye): cell nuclei. Scale bar: 100 µm

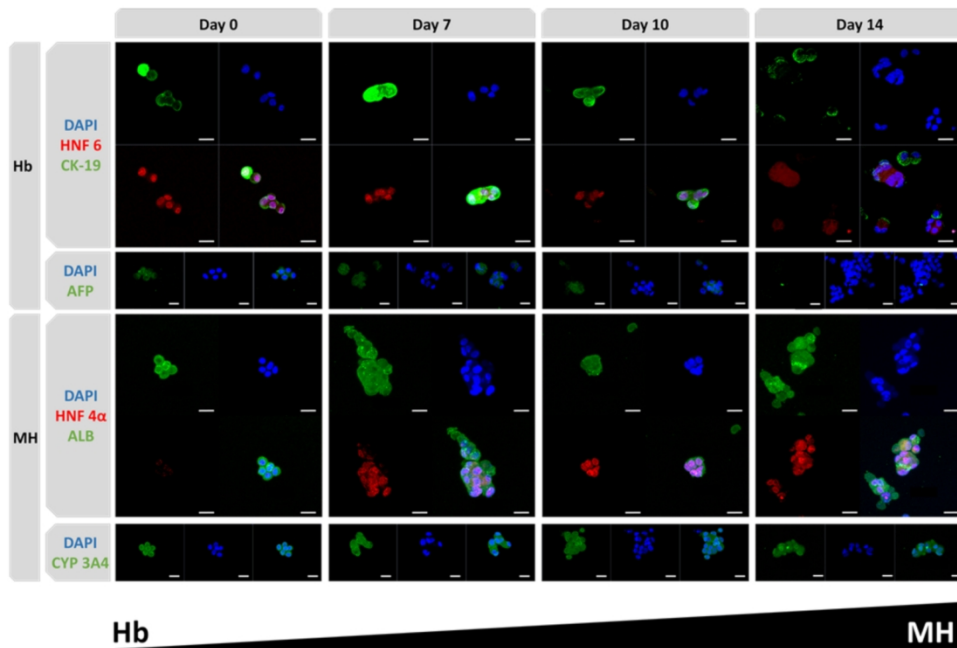
99x69mm (300 x 300 DPI)

1
2
3
4
5
6
7
8
9
10
11
12
13
14
15
16
17
18
19
20
21
22
23
24
25
26
27
28
29
30
31
32
33
34
35
36
37
38
39
40
41
42
43
44
45
46
47
48
49
50
51
52
53
54
55
56
57
58
59
60



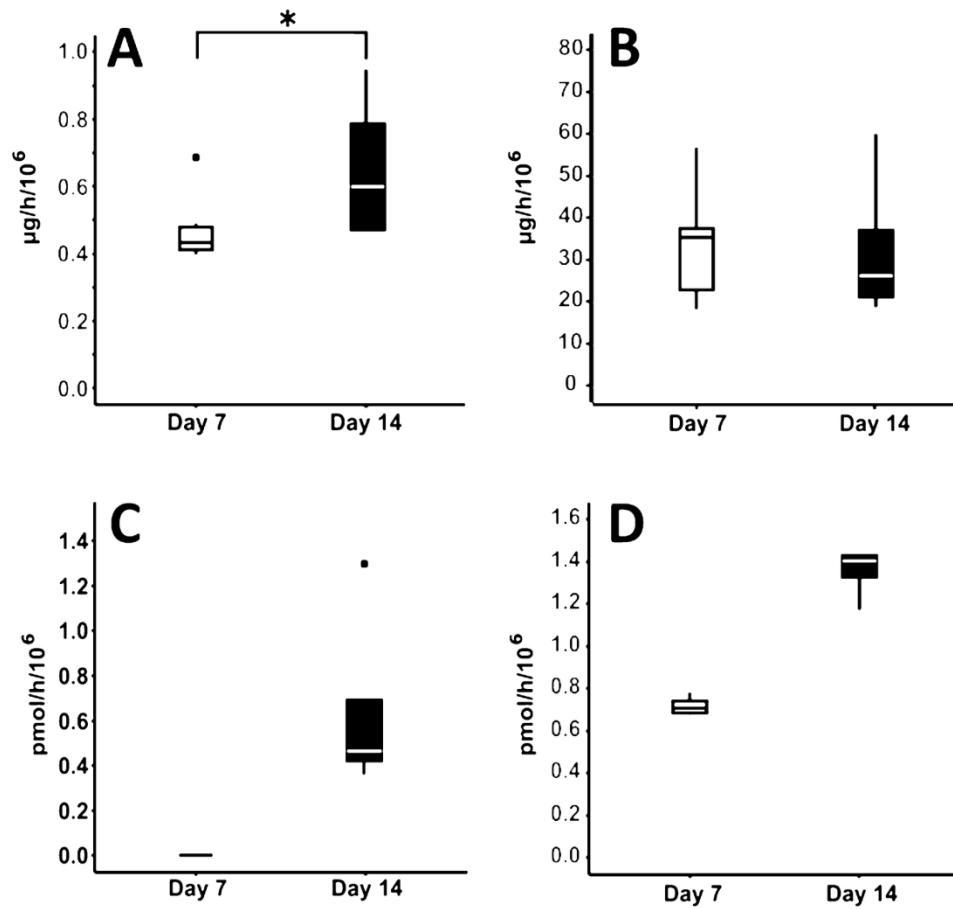
cells self-rearranged in aggregates: diameters over time (A). F-actin (phalloidin, in green) and nuclei (DAPI, in blue) staining at day 14 (B) (confocal microscopy). Scale bar: 20 μm

159x52mm (300 x 300 DPI)



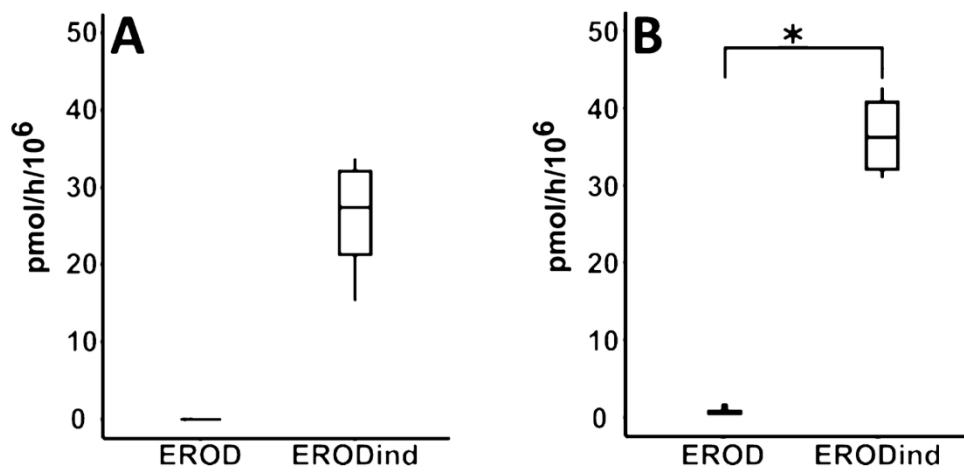
immunofluorescence staining over time (confocal microscopy). Hepatoblast markers (Hb): HNF 6 in red, CK-19 in green, AFP in green, nuclei in blue. Mature hepatocyte markers (MH): HNF 4α in red, ALB in green, CYP 3A4 in green, nuclei in blue. Scale bar: 20 μm

139x95mm (300 x 300 DPI)



metabolic activities of encapsulated cells at day 7 and day 14. Albumin secretion rate (A, significance analysed by Wilcoxon matched-pairs signed-ranks test), ICG releasing rate by the transporters MDR3 and MRP2 (B), CYP1A1/2 activity (C), CYP3A4 activity (D)

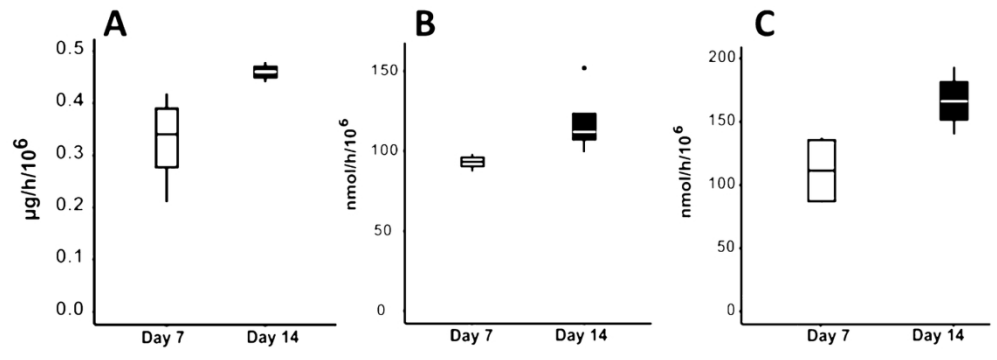
160x154mm (300 x 300 DPI)



CYP1A1/2 activity after induction by β -naphthoflavone 100 μ M and rifampicin 10 μ M at day 7 (A) and 14 (B), significance analysed by Mann-Whitney Test

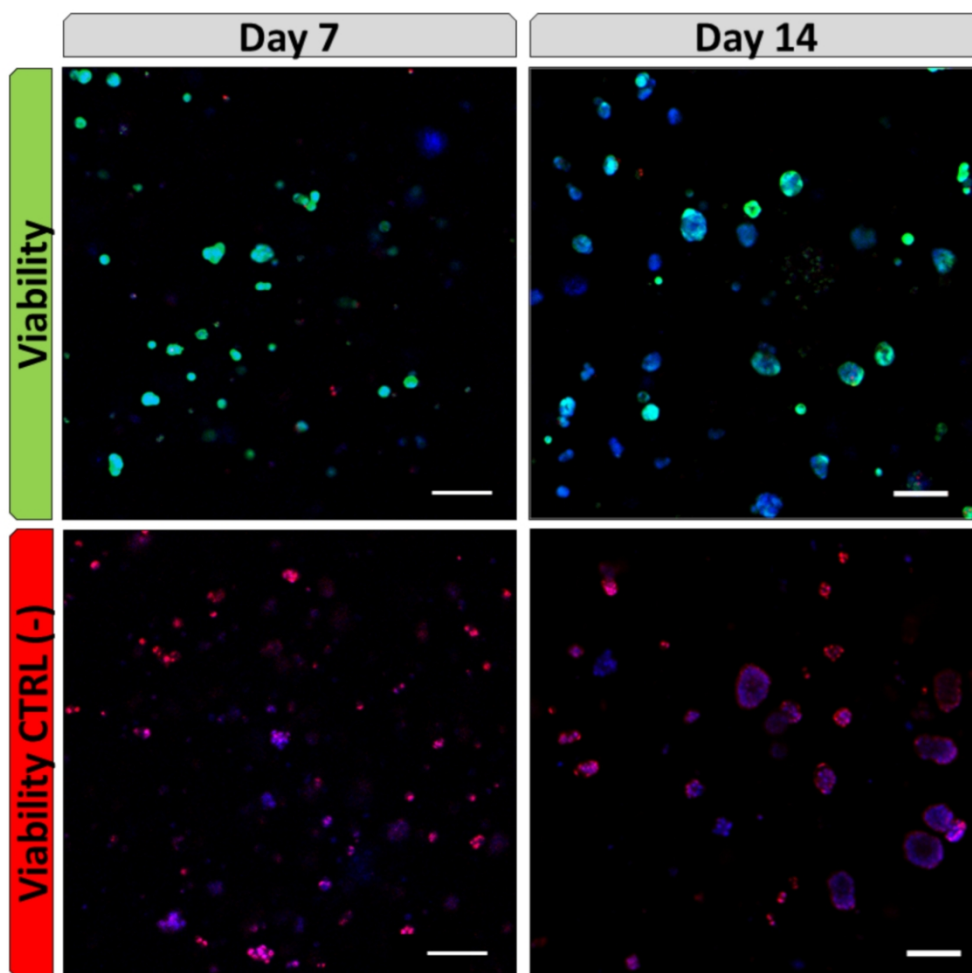
160x80mm (300 x 300 DPI)

1
2
3
4
5
6
7
8
9
10
11
12
13
14
15
16
17
18
19
20
21
22
23
24
25
26
27
28
29
30
31
32
33
34
35
36
37
38
39
40
41
42
43
44
45
46
47
48
49
50
51
52
53
54
55
56
57
58
59
60



metabolic activities of encapsulated cells in BAL function test medium at day 7 and 14. Albumin synthesis rate (A), ammonia (B) and lactate (C) detoxification rate

159x58mm (300 x 300 DPI)



cell viability after exposition to BAL function test medium at day 7 and 14 (confocal microscopy). In green (Calcein AM): viable cells, in red (ethidium homodimer-1): dead cells, in blue (Hoechst 33342 dye): cell nuclei. Scale bar: 100 μ m

99x99mm (300 x 300 DPI)

1. Supplementary

In a preliminary study, pre-formed spheroids were generated in order to test their metabolic performance at day 7. In particular, after cell amplification in 2D monolayers, cells at passage 18 were detached, mixed with the alginate solution at density of 5×10^6 cells per mL and encapsulated. In order to obtain cell spheroids, 5×10^6 cells were inoculated in glass culture dishes (50 mm x 15mm), coated with an anti-adhesive coating (Sigmacote[®], SL2 Sigma-Aldrich). Cells were subjected to continuous orbital agitation at 60 rpm with oscillation amplitude of 16 mm (SSL1 orbital shaker, Stuart) in a humidified environment at 37°C and 5% CO₂. Proliferation culture medium was replaced one time during the spheroid's formation. After 3 days of aggregation, spheroids were encapsulated. Aggregate size was determined by measuring Feret's diameter using ImageJ software version 1.52h.

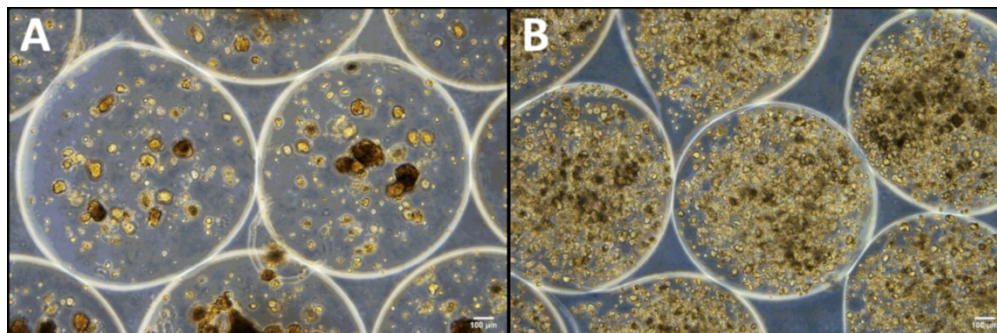
Here we report a comparison between the diameter of pre-formed spheroids and the spheroids formed inside the beads, discussed in this article, at day 7 (figure 1 and 2 supplementary data).

Figure 1 supplementary

Figure 2 supplementary

The analyses carried out at day 7 post-encapsulation, show that the cell density (recorded by DNA quantification) and the metabolic activities of the two experimental setups remain equivalent (data not shown). Since working with pre-formed spheroids is complicated in logistical terms (especially the scaling-up for human applications), we opted to work with directly encapsulated cells that rearrange into spheroids within the beads.

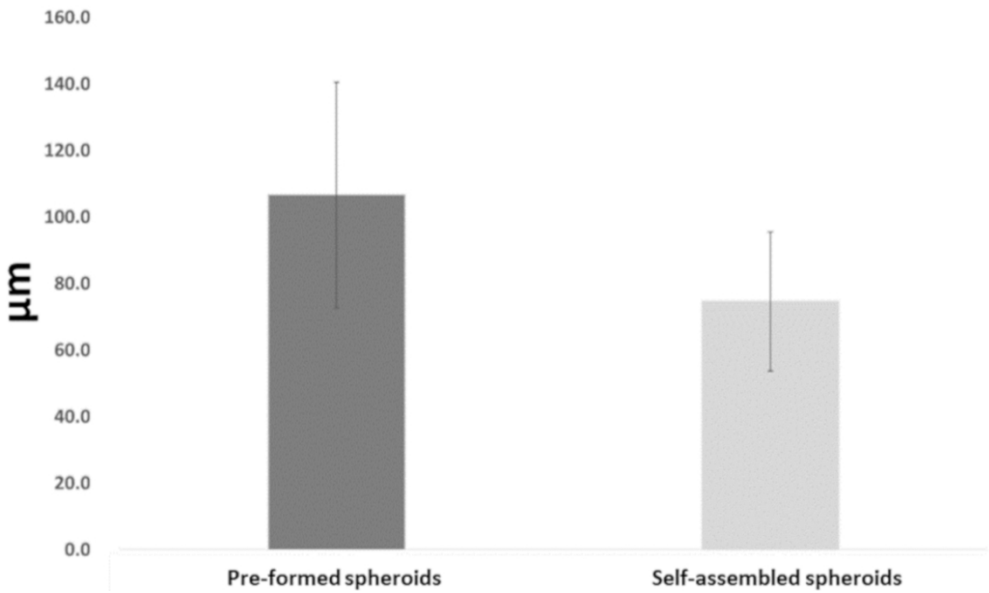
1
2
3
4
5
6
7
8
9
10
11
12
13
14
15
16
17
18
19
20
21
22
23
24
25
26
27
28
29
30
31
32
33
34
35
36
37
38
39
40
41
42
43
44
45
46
47
48
49
50
51
52
53
54
55
56
57
58
59
60



pre-formed spheroids (A) and cells in beads rearranged in spheroids (B) (bright field microscopy). Scale bar: 100 μm

109x36mm (300 x 300 DPI)

1
2
3
4
5
6
7
8
9
10
11
12
13
14
15
16
17
18
19
20
21
22
23
24
25
26
27
28
29
30
31
32
33
34
35
36
37
38
39
40
41
42
43
44
45
46
47
48
49
50
51
52
53
54
55
56
57
58
59
60



diameter of pre-formed spheroids and cells in beads rearranged in spheroids at day 7 post-encapsulation

99x59mm (300 x 300 DPI)